A&A 531, L2 (2011)
DOI: 10.1051/0004-6361/201116796

Astronomy & Astrophysics

Letter to the Editor

High-sensitivity search for clumps in the Vega Kuiper-belt

New PdBI 1.3 mm observations⋆,⋆⋆

V. Piétu[1], E. Di Folco[2,3], S. Guilloteau[4,5], F. Gueth[1], and P. Cox[1]

[1] IRAM, 300 rue de la piscine, 38406 Saint Martin d'Hères, France
e-mail: pietu@iram.fr
[2] CEA Saclay/Service d'Astrophysique, Laboratoire AIM, CEA/DSM/IRFU-CNRS-Université Paris Diderot, 91191 Gif-sur-Yvette Cedex, France
[3] LESIA-UMR 8109, CNRS and Observatoire de Paris-Meudon, 5 place J. Janssen, 92195 Meudon, France
[4] Université de Bordeaux, Observatoire Aquitain des Sciences de l'Univers, 2 rue de l'Observatoire BP 89, 33271 Floirac, France
[5] CNRS/INSU – UMR5804, Laboratoire d'Astrophysique de Bordeaux, 2 rue de l'Observatoire BP 89, 33271 Floirac, France

Received 27 February 2011 / Accepted 27 April 2011

ABSTRACT

Context. Previous studies have found that Vega is surrounded by an extended debris disc that is very smooth in the far infrared, but displays possible clumpiness at 850 μm and dust emission peaks at 1.3 mm.
Aims. We reobserved Vega at 1.3 mm with PdBI to constrain its circumstellar dust distribution.
Methods. Our observations of a three-field mosaic have a factor of two higher sensitivity than previous observations.
Results. We detect Vega photosphere with the expected flux, but none of the previously reported emission peaks that should have been detected at the >6σ level, with a sensitivity <1 mK.
Conclusions. This implies that the dust distribution around Vega is principally smooth and circularly symmetric. This also means that no planet is needed to account for dust trapped in mean-motion resonnance.

Key words. radio continuum: stars – stars: individual: Vega – circumstellar matter – methods: observational – instrumentation: interferometers

1. Introduction

More than 25 years after the first debris discs were discovered by the IRAS mission (Aumann et al. 1984; Aumann 1985), the presence of Edgeworth-Kuiper belts around other stars has been widely attested. Statistical studies conducted with the Spitzer satellite on large samples of main sequence stars have shown that 30 ± 5% of A type and 16 ± 3% of FGK type stars exhibit detectable IR excess emission longward of 24 μm (Su et al. 2006; Bryden et al. 2006; Trilling et al. 2008). This excess luminosity is attributed to the presence of cold dust grains arranged in a disc or ring(s). Among those, only a handful of nearby systems have been resolved because of obvious limitations in sensitivity and angular resolution. Being one of the first systems detected, Vega (A0V, 7.76 pc) has a particular status, and is usually considered as a prototype of debris discs stars.

Given its proximity to the Earth, its face-on disc has been successfully imaged from IR to mm-wavelengths. Its appearance curiously seems to change from a smooth azimuthal profile at short wavelengths to a more structured, clumpy ring in the sub-mm domain. MIPS images at 24, 70 and 160 μm (Su et al. 2005) show circular profiles, the emission being detected up to 815 AU for the latter. The radial profile analysis suggests a ring-like distribution of material (after subtraction of the photosphere contribution), with an inner boundary located around 85 ± 15 AU. *Herschel*/PACS observations at 70 and 160 μm directly confirmed this ring morphology, with a peak intensity occuring at 85 AU (Sibthorpe et al. 2010), as well as the smooth brightness profile.

At sub-mm wavelengths, the first image was reported by Holland et al. (1998) with JCMT/SCUBA at 850 μm. The resolved emission extents to scales twice as large as our Solar System, with a possible peak emission located at ~70 AU, northeast of the star, accounting for less than 40% of the total flux. The possible asymmetry of their map, although at the 2σ level, has motivated several subsequent studies to explore the nature of the blob and its putative link with unseen planets. Koerner et al. (2001) observed Vega with OVRO at 1.3 mm and reported a ring arc located at 95 AU (12″ from the star). Wilner et al. (2002) used the Plateau de Bure Interferometer (IRAM) to probe the continuum emission at 1.3 and 3.3 mm. While the star was only detected at the former wavelength, no peak emission appeared in the original resolution map. Degrading the interferometer resolution, Wilner et al. (2002) claimed that extended exists emission concentrated in two blobs located at 8 and 9.5″ (60 and 75 AU), southwest and northeast of the star respectively. Using the SHARC II camera at CSO, Marsh et al. (2006) detected ring-like structures of the 350 μm and 450 μm emissions, with some inhomogeneity at the 2–4σ level. The brightness peaks in the

⋆ Based on observations carried out with the IRAM Plateau de Bure Interferometer. IRAM is supported by INSU/CNRS (France), MPG (Germany) and IGN (Spain).
⋆⋆ Processed data from Fig. 1 are only available at the CDS via anonymous ftp to cdsarc.u-strasbg.fr (130.79.128.5) or via http://cdsarc.u-strasbg.fr/viz-bin/qcat?J/A+A/531/L2

Table 1. Description of the fields observed and point-source fit.

Field	RA Off. (")	Dec Off. (")	Noise (mJy)	Fit. RA (")	Fit. Dec (")	Flux (mJy)	Corr. Flux (mJy)
North-East	3	5	0.26	0.13 ± 0.16	0.30 ± 0.14	1.70 ± 0.23	2.05 ± 0.28
South-West	–3	–5	0.29	–0.12 ± 0.19	0.03 ± 0.16	1.48 ± 0.23	1.81 ± 0.28
Central	0	0	0.37	–0.70 ± 0.15	–0.01 ± 0.16	1.96 ± 0.32	1.98 ± 0.32

Notes. From left to right, the columns are: Col. 1: field name; Cols. 2, 3: field pointing center (offsets from α = 18:36:56.330, δ = 38:47:01.30, J2000.0); Col. 4: noise in the field; Cols. 5–8: fit of point-source; Cols. 5, 6: fitted positions are offsets from α = 18:36:56.359, δ = 38:47:01.20 (after correction for proper motion – see text); Cols. 7, 8: fitted flux, and flux corrected for primary beam attenuation.

photosphere-subtracted images partially overlap with those reported at 850 μm and 1.3 mm, strongly suggesting that grains and/or planetesimal concentrations exist in the belt around Vega.

The possible existence of concentrations in the dust belt has long been interpreted (and modelled) as the evidence of grains trapped in mean-motion resonances (MMR) with a putative, but unseen, massive planet located close to the inner radius of the planetesimal ring (Holland et al. 1998; Wilner et al. 2002; Wyatt 2003). Two scenarios have been invoked to populate the MMRs with an unseen planet: the particles are trapped either while migrating inward under the influence of Poyinting-Robertson (P-R) drag (e.g. Kuchner & Holman 2003), or during the outward migration of the planet itself. Models developed by Wyatt (2003) and Reche et al. (2008) invoke the outward migration of a Neptune- to Saturn-mass planet in a circular (and elliptical, respectively) orbit to reproduce the observed clumps. To reconcile the different views of the disc morphology at the different wavelengths, it has been suggested that the clumps seen in the sub-mm trace large grains trapped in the same resonance as their parent planetesimals, while intermediate and small grains (down to the blown-out size) are decoupled from the resonant structure, thus forming a smooth and axisymmetric disc component observed at shorter wavelengths. This broad and smooth halo could therefore be sculpted by small grains evacuated from the MMRs by the stellar radiation pressure (Wyatt 2006) and/or by the high-velocity collisions between their parent planetesimals (Krivov et al. 2007). Substantial observational efforts have been invested in the quest for the predicted planet(s), mostly based on near-IR adaptive optics (and/or coronagraphic) techniques on large telescopes (Marois et al. 2006; Hinz et al. 2006). This search remains unsuccessful today, essentially because of the lack of sensitivity at the predicted planet position (7–10″).

The Vega system thus appears to be a unique laboratory for constraining and understanding the evolution of dust grains in exo-Kuiper belts, in particular the interaction between planetesimals, grains, and planets.

2. Observations and analysis

2.1. Observations

During the winter 2006/07, a new generation of receivers was installed on the Plateau de Bure interferometer, enabling single frequency dual-polarization observations with improved noise figures, single-side band tuning and larger bandwidth. This instrumental upgrade resulted in a significantly improved sensitivity of the array (at 1.3 mm, the total gain was an increase by a factor of four in continuum sensitivity). As part of the science verification program, Vega was observed in January 2007 at 230.538 GHz. These observations were carried in the D (compact) configuration of the PdBI (with baselines ranging from 15 to 85 m, the most suited arrangement for detecting large scale emission). The tuning was in the lower side-band (LSB), with $T_{\rm rec} \sim 50$ K and a bandwith of 850 MHz in each of the two orthogonal linear polarizations (H and V). The atmospheric phase noise ranged from 20 to 50°. Despite these first observations reaching a sensitivity comparable to that of Wilner et al. (2002), we detected only the central point source, but no extended emission at all.

We thus reobserved a two-field mosaic towards Vega (offset by (3, 5″) and (–3, –5″), respectively, the primary beams being indicated in Fig. 1 together with the central pointing obtained in January) in October and November 2007, again in the D configuration and with the same spectral setup. Atmospheric phase noise was again between 20° and 50°. The absolute flux calibration was performed using observation of MWC349. Its flux density model has recently been revised at IRAM, with a 16% increase in flux (Krips et al., in prep.), so we used 1.98 Jy as a flux model at 230.5 GHz. With a grand-total observing time of 16 h on source, we finally reach a sensitivity limit below 0.2 mJy/beam (0.9 mK with natural weighting) in the central region of the final mosaic map, and <0.4 mJy/beam within 11″ from Vega.

2.2. Analysis

Vega has a high proper motion (μ_α = 201.03 mas/yr, μ_δ = 287.47 mas/yr, with an error ellipse of 0.63 × 0.54 mas/yr, at PA 144°, Perryman et al. 1997). We corrected the individual (u,v) tables for proper motion using the value of Perryman et al. (1997) to a common J2000.0 Equinox prior to data analysis.

We then performed point-source fits in the (u,v) plane and detected a point source in each of the fields. The fitted position agrees within the error bars (see Table 1), as does the flux density, when we take into account the attenuation by the primary beam for the offset fields. The mean value is 1.95 ± 0.17 mJy. Wilner et al. (2002) found 1.7 ± 0.30 mJy[1], but used 1.70 Jy as a flux density for MWC349. Correcting for the calibrator flux difference, their flux becomes 1.98 ± 0.35 mJy, in excellent agreement with our measurement. This is consistent with the 2.11 mJy value expected from the pole-on photosphere for which we refer to the modelling by Müller et al. (2010), who took into account the discrepancy between the polar and equatorial temperature resulting from the fast spin velocity of this star.

Data were processed with GILDAS software[2] using the classical mosaicing algorithm (see e.g. Gueth & Guilloteau 2000). We present the resulting continuum maps in Fig. 1: in the top row we present maps obtained with natural weighting, while in

[1] They cite 1.7 ± 0.13 mJy from a Gaussian fit, but the error in a point source flux cannot be below the rms noise of the image, which they indicate is 0.3 mJy/beam.

[2] See `http://www.iram.fr/IRAMFR/GILDAS` for more information about GILDAS.

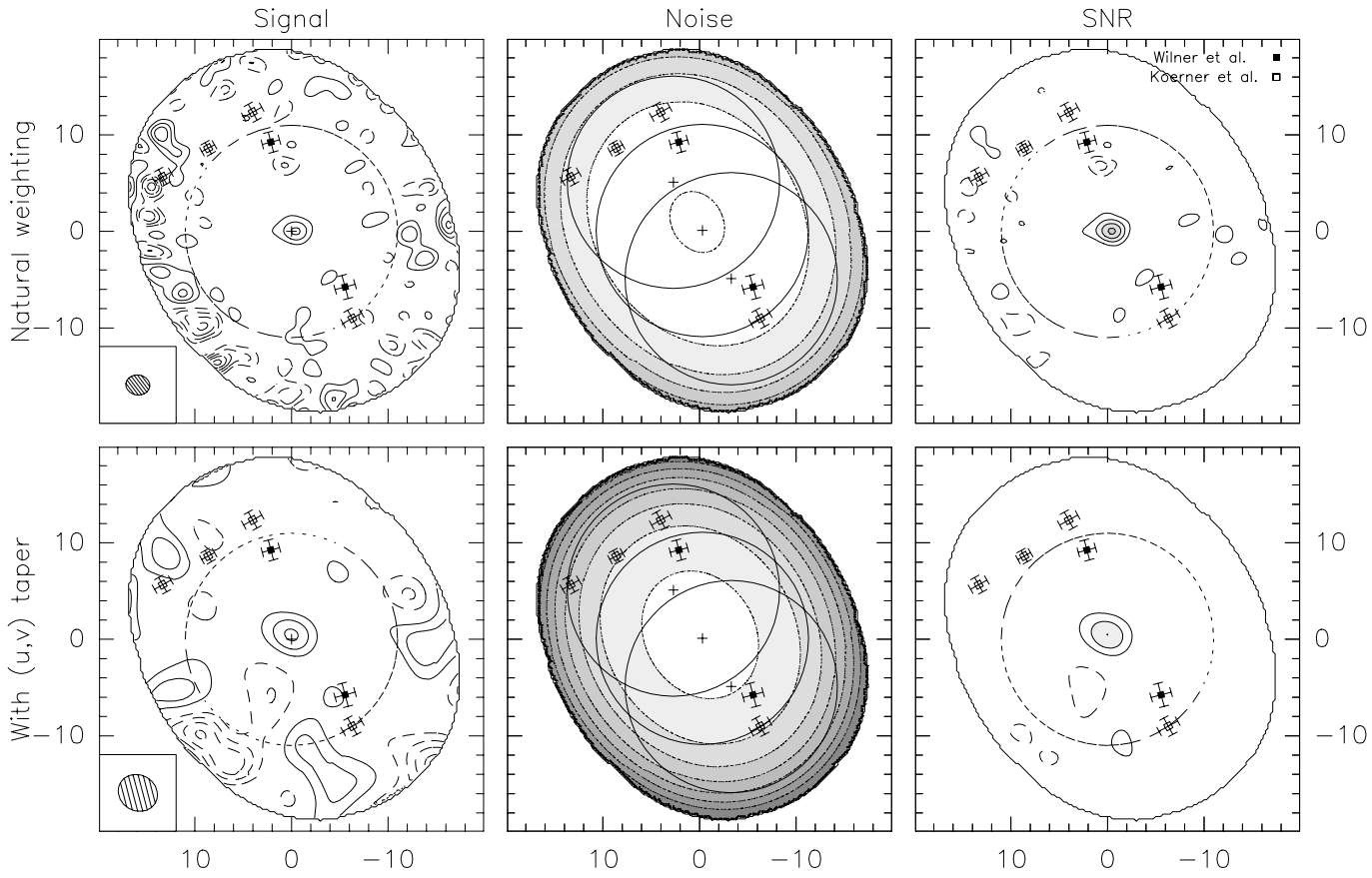

Fig. 1. *Top left*: natural weighting 1.3 mm continuum image (corrected for the primary beam attenuation). The angular resoluion is $2.5 \times 2.1''$ at PA 82° and the contour spacing 0.5 mJy/beam (2.1 mK), with negative contours being dashed. The dashed circle represents the primary-beam half-power field of view. *Top center*: corresponding noise map. Contour spacing is 0.2 mJy/beam. The circles show the observed individual fields (half-power field of view, centered on the crosses). *Top right*: signal-to-noise ratio map. Contour spacing is 2σ. *Bottom left*: 1.3 mm continuum image obtained with a (u, v) taper. Angular resolution is $4.2 \times 3.7''$ at PA 60° and contour spacing is 0.6 mJy/beam (0.8 mK). *Bottom center*: corresponding noise map. Contour spacing is 0.2 mJy/beam (with the first contour being at 0.4 mJy/beam). *Bottom right*: signal-to-noise ratio map. Contour spacing is 2σ. In all maps, the filled square symbols indicate the location of the extended emissions found by Wilner et al. (2002) and the empty square symbols indicate the location of the peaks reported by Koerner et al. (2001). North is up, and east to the left.

the bottom row the data have been tapered in the (u,v) plane (with elliptical Gaussian $1/e$ widths of 30×40 m at PA 0°) to increase the sensitivity to putative extended emission by degrading the angular resolution. Since the mosaicing algorithm produces images corrected for the primary beam attenuation, the noise increases towards the map's edges (as is clearly visible in the signal maps in the left column of Fig. 1). We present in the middle column of Fig. 1 the corresponding noise maps that show our sensitivity limit as a function of the position in the field of view. The right column of Fig. 1 shows the signal-to-noise ratio maps obtained in each case by dividing of the signal map by the noise map. From these, we conclude that only the central point source is detected with a $SNR > 3$.

2.3. Comparison with previous work

Previous interferometric observations at 1.3 mm were reported by Koerner et al. (2001) and Wilner et al. (2002). With an angular resolution of $3.3 \times 2.9''$, Koerner et al. (2001) found an arc ring at 95 AU with four peaks located between 11 and 14.5″ of flux density ranging from 2.4 to 4.0 mJy (3 to 4σ level) after correcting for primary beam attenuation. In addition to the central point source, Wilner et al. (2002) reported two emission peaks located at 8.0 and 9.5″, after tapering their data to a $5.3 \times 4.6''$ resolution. From a Gaussian fit in the *(u,v)* plane, they obtained fluxes (corrected for the primary beam attenuation) of 7.1 ± 1.4 and 4.3 ± 1.0 mJy, respectively (4 to 5σ level). The position of these dust peaks is reported in Fig. 1, with their 1σ error ellipse derived from the signal-to-noise ratio and synthesized beam. These two results clearly do not agree, as none of the error ellipse overlap. We also note that the comparison of the different results need to take into account that their single field maps are not corrected for primary beam attenuation, in contrast to the maps we present here.

At the position of the peaks reported by Koerner et al. (2001), our observations have a 1σ sensitivity of 0.35 mJy/beam (0.54 for the most distant peak), a factor of between two and three better than the OVRO observations. If real, these peaks should have been detected at the $>6-8\sigma$ level. Similarly, our observations reach a 1σ sensitivity limit of 0.26 mJy/beam (1.1 mK) or 0.45mJy/beam (0.6 mK) at the position of the Wilner et al. (2002) peaks for the untapered and tapered maps, respectively. Thus, depending on their size, the two structures should have been detected at the $10-15\sigma$ and $6-10\sigma$ level in our maps.

Among the possible ways of explaining our non-detection, we exclude calibration errors since we detect the central source, at the expected position and with the expected flux, which is an excellent internal quality check. Given the above-mentioned flux calibration scaling with respect to the Wilner et al. (2002) data, any supposed bias in the flux calibrationshould enhance

the probability of detecting the blobs in our maps, since their intensity should also be higher by 16%. If these structures had rotated according to Keplerian motion, the displacement within the ~6 year interval would have been smaller than 1″.

3. Discussion

Our PdBI observations are consistent with no detectable millimetric emission from the outer dusty disc (or ring) surrounding Vega. We briefly discuss the impact of this new constraint on the dust properties in this system.

3.1. Clumpiness

We have shown in Sect. 2.3 that the clumps previously reported at 1.3 mm by Koerner et al. (2001) and Wilner et al. (2002) are not detected in our observations, which are deeper in sensitivity by a factor of two, and are probably low-significance artifacts. A trivial implication of this finding is that no planet is required to trap dust in mean-motion resonance at these positions. More generally, our results also shed new light on the clumpiness of the dust surrounding Vega. Observations at shorter wavelengths display very smooth images (Su et al. 2005; Sibthorpe et al. 2010) and the asymmetry of the 850 μm image is only at the 2σ level, hence also compatible with a smooth dust distribution (Holland et al. 1998). The only detection of a possible asymmetry comes from the SHARC II images at 350 and 450 μm (Marsh et al. 2006) but is at the $2-4\sigma$ and <10% of the ring brightness. In conclusion, all observations display or are compatible with a smooth dust distribution.

3.2. Upper limit on the disc emission at 1.3 mm

Earlier sub-mm observations have convincingly established the existence of an extended emission around Vega, with a ring-like morphology at 350 μm, 450 μm with CSO SHARC II (Marsh et al. 2006), and 70−160 μm with *Herschel*/PACS (Sibthorpe et al. 2010). According to these studies, the peak intensity is located around 85−100 AU (11−13″). To set an upper limit on the 1.3 mm emission of this ring, we fitted a thin, uniform, 85 AU radius ring into the *(u,v)* data, carefully taking into account the different fields of the mosaic (for numerical reasons, this thin ring is represented by an adequately sampled series of point sources). We find an integrated flux of 0.1 ± 2.0 mJy, i.e. a 3σ upper limit of 6 mJy. The lack of clear detection at high angular resolution relative to the bolometer results, which are more sensitive to extended flux, suggests that a thin ring may not be the most appropriate distribution. If we instead assume a uniform annulus of inner radius 85 AU and outer radius 105 AU, we find an integrated flux of -5.3 ± 2.4 mJy, i.e., a 3σ upper limit of 7.2 mJy, which is similar to the narrow ring value.

Using the Sibthorpe et al. (2010) model, with an inner Gaussian and outer exponential decline in surface brightness (with a transition radius of 14″), our results are compatible with a total flux <24 mJy (3σ) if the distribution is truncated at 200 AU, and <30 mJy if it extends up to 300 AU. This modelling also agrees with the 3σ upper limit of 6 mJy for emission within 105 AU. With this model, we are clearly unable to place strong constraints on the dust properties, since our data lack sensitivity to faint extended emission.

Assuming a dust temperature of 68 K (Sheret et al. 2004) and a dust absorption coefficient of 0.5 cm^2 g^{-1} (Natta et al. 2004), our 3σ flux density limit of 6 mJy translates into an upper limit on the dust grain mass in the ring of $M_{\rm dust} = 0.8\ M_{\rm moon}$ (or $10^{-2}\ M_{\oplus}$, not taking into account the parent bodies). With the Sibthorpe et al. (2010) model, the upper limit on the total dust grain mass is 3.9 $M_{\rm moon}$. This upper limit is consistent with the maximum dust mass obtained by Müller et al. (2010) in their modelling of the Vega disc as a steady-state collisional cascade.

The best fit of the dust spectral energy distribution using measurements of Sibthorpe et al. (2010) and Holland et al. (1998), corrected for the stellar emission, gives a spectral index of 2.9 and results in an extrapolated flux at 1.3 mm of 12 mJy. Our upper limit hence agrees with the measurements made at shorter wavelengths.

4. Conclusions

Taking advantage of new receivers at IRAM Plateau de Bure Interferometer, we have probed the Vega debris disc to investigate in depth the possible presence of clumps in the well-known dust belt. Apart from the stellar photosphere, we have detected neither a point-source nor extended emission in our three-field mosaic, although our sensitivity limit at 1.3 mm has improved by a factor of two compared to earlier studies. In particular, we have found no evidence for the northeast and southwest blobs claimed by Koerner et al. (2001) or Wilner et al. (2002). These structures, which had been interpreted as the signature of the gravitational influence of putative unseen planets, should have been detected in our interferometric map at the >6σ level.

The upper limits that we have derived on both the emission of a narrow ring extended emission are compatible with observations at shorter wavelenghts. All observations indicate that the disc/ring system surrounding Vega is smooth and circularly symetric, hence do not require the gravitational influence of a giant planet to sculpt asymmetries in the disc, at the current level of detection.

Acknowledgements. We acknowledge help from the Plateau de Bure staff when carrying out the observations. We thank our anonymous referee for helpful comments.

References

Aumann, H. H. 1985, PASP, 97, 885
Aumann, H. H., Beichman, C. A., Gillett, F. C., et al. 1984, ApJ, 278, L23
Bryden, G., Beichman, C. A., Rieke, G. H., et al. 2006, ApJ, 646, 1038
Gueth, F., & Guilloteau, S. 2000, in Imaging at Radio through Submillimeter Wavelengths, ed. J. G. Mangum, & S. J. E. Radford, ASP Conf. Ser., 217, 291
Hinz, P. M., Heinze, A. N., Sivanandam, S., et al. 2006, ApJ, 653, 1486
Holland, W. S., Greaves, J. S., Zuckerman, B., et al. 1998, Nature, 392, 788
Koerner, D. W., Sargent, A. I., & Ostroff, N. A. 2001, ApJ, 560, L181
Krivov, A. V., Queck, M., Löhne, T., & Sremčević, M. 2007, A&A, 462, 199
Kuchner, M. J., & Holman, M. J. 2003, ApJ, 588, 1110
Marois, C., Lafrenière, D., Doyon, R., Macintosh, B., & Nadeau, D. 2006, ApJ, 641, 556
Marsh, K. A., Dowell, C. D., Velusamy, T., Grogan, K., & Beichman, C. A. 2006, ApJ, 646, L77
Müller, S., Löhne, T., & Krivov, A. V. 2010, ApJ, 708, 1728
Natta, A., Testi, L., Neri, R., Shepherd, D. S., & Wilner, D. J. 2004, A&A, 416, 179
Perryman, M. A. C., Lindegren, L., Kovalevsky, J., et al. 1997, A&A, 323, L49
Reche, R., Beust, H., Augereau, J., & Absil, O. 2008, A&A, 480, 551
Sheret, I., Dent, W. R. F., & Wyatt, M. C. 2004, MNRAS, 348, 1282
Sibthorpe, B., Vandenbussche, B., Greaves, J. S., et al. 2010, A&A, 518, L130
Su, K. Y. L., Rieke, G. H., Misselt, K. A., et al. 2005, ApJ, 628, 487
Su, K. Y. L., Rieke, G. H., Stansberry, J. A., et al. 2006, ApJ, 653, 675
Trilling, D. E., Bryden, G., Beichman, C. A., et al. 2008, ApJ, 674, 1086
Wilner, D. J., Holman, M. J., Kuchner, M. J., & Ho, P. T. P. 2002, ApJ, 569, L115
Wyatt, M. C. 2003, ApJ, 598, 1321
Wyatt, M. C. 2006, ApJ, 639, 1153